Computing Call Blocking Probabilities in LEO Satellite Networks: The Single Orbit Case

A. Halim Zaim George N. Rouskas Harry G. Perros

TR-2000-06

June 19, 2000

Abstract

We study the problem of carrying voice calls over a LEO satellite network, and we present an analytical model for computing call blocking probabilities for a single orbit of a satellite constellation. We have devised a method to solve the corresponding Markov process efficiently for up to 5-satellite orbits. For orbits consisting of a larger number of satellites, we have developed an approximate decomposition algorithm to compute the call blocking probabilities by decomposing the system into smaller sub-systems, and iteratively solving each sub-system in isolation using the exact Markov process. Our approach can capture blocking due to hand-offs for both satellite-fixed and earth-fixed constellations. Numerical results demonstrate that our method is accurate for a wide range of traffic patterns and for orbits with a number of satellites that is representative of commercial satellite systems.

Keywords: Low earth orbit satellite networks, call blocking probability, hand-offs, decomposition algorithms

Department of Computer Science
North Carolina State University
Raleigh, NC 27695-7534

1 Introduction

Currently, we are witnessing an increase in the demand for a broad range of wireless telephone and internet services. Satellite based communication is posed to provide mobile telephony and data transmission services on a worldwide basis in a seamless way with terrestrial networks. Satellite systems are location-insensitive, and they can be used to extend the reach of networks and applications to anywhere on the earth.

Satellites can be launched in different orbits, of which, the low earth orbit (LEO), the medium earth orbit (MEO), and the geo-stationary orbit (GEO), are the most well-known. LEO satellites are placed in orbits at an altitude of less than 2000 km above the earth. Their orbit period is about 90 minutes, and the radius of the footprint area of a LEO satellite is between 3000 km to 4000 km. The duration of a satellite in LEO orbit over the local horizon of an observer on earth is approximately 20 minutes, and the propagation delay is about 25ms. A few tens of satellites on several orbits are needed to provide global coverage. MEO satellites are placed in circular orbits at an altitude of around 10000 km. Their orbit period is about six hours, and the duration of a satellite in MEO orbit over the local horizon of an observer on earth is a few hours. Fewer satellites on two or three orbits is enough to provide a global coverage in a MEO system. Propagation delay in a MEO system is about 125ms. GEO satellites are also in circular orbits in the equatorial plane at an altitude of 35786 km, with an orbital period equal to that of the earth. A satellite in GEO orbit appears to be fixed above the earth's surface. The footprint of a GEO satellite covers nearly one third of the earth's surface (between 75^o south to 75^o north). Therefore, a near global coverage can be obtained with three satellites, but the propagation delay is 250 ms.

A LEO or MEO satellite system is a set of identical satellites, launched in several orbital planes with the orbits having the same altitude. The satellites move in a synchronized way in trajectories relative to the earth. Such a set of satellites is referred to as a *constellation* of satellites. The position of all the satellites in relation to the earth at some instance of time, repeats itself after a predetermined period which is usually several days, while a satellite within an orbit also comes to the same point on the sky relative to the earth after a certain time.

In a LEO or MEO satellite system, satellites can communicate directly with each other by line of sight using intraplane inter-satellite links (ISL) which connect satellites in the same orbital plane and interplane ISLs which connect satellites in adjacent planes. ISLs introduce flexibility in routing, they can be used to build in redundancy into the network, and they permit two users in different footprints to communicate without the need of a terrestrial system. To improve the bandwidth and frequency efficiency, the satellite footprint area is divided into smaller cells. For each cell within a footprint, a specific beam of the satellite is used. A constellation of satellites may provide either *satellite-fixed* cell coverage or *earth-fixed* cell coverage. In the first case, the satellite antenna sending the beam is fixed, and as the satellite moves along its orbit, its footprint and the cell move as well. In the case of earth-fixed cell coverage, the earth surface is divided into cells, as in a terrestrial cellular system, and a cell is serviced continuously by the same beam during the entire time that the cell is within the footprint area of the satellite.

As satellites move, fixed and mobile users hand off from one beam to another (beam hand-off) or from

one satellite to another (satellite hand-off). The velocity of a satellite is much higher than the velocity of objects on earth. Therefore, the number of hand-offs during a telephone call depends on the call duration, the beam size, the satellite footprint size and the satellite speed, while the location and mobility of a user only effects the time a hand-off takes place. For example, for a call duration of 3 min., the customer of a LEO satellite constellation with an elevation angle of 10^o, will experience two hand-offs. In an earth-fixed system, each beam is assigned to a fixed cell on the earth within the satellite's footprint. During a satellite hand-off, all beams are reassigned to their respective cells in the adjacent footprint area. Therefore, in these systems, both beam and satellite hand-offs occur at the same time. In a satellite-fixed system, a user may be handed off to the next beam in the same satellite or the satellite behind, as the cell defined by the beam moves away from the user. The newly entered beam, may or may not have enough bandwidth to carry the handed-off traffic. In the case of satellite-based telephony, the new beam may not be able to carry a handed-off telephone call, in which case, the call will be dropped. In general, hand-offs in satellite systems impose a big problem from the point of quality of service.

There are several LEO systems currently in operation, such as Argos, VITAsat, ORBCOMM, and Globalstar. Several others, such as LEOone, SkyBridge, and Teledesic, are scheduled to start after 2000. These systems differ in many aspects, including the number of orbits and the number of satellites per orbit, the number of beams per satellite, their capacity, the band they operate (K-Band, Ka-Band, L-Band, etc.), and the access method employed (FDMA, TDMA, or CDMA). Also, these systems provide different services and they may or may not have on-board switching capabilities. For instance, Iridium provides telephone service only, LEOone will provide data communications only, while most other satellite systems are designed to provide multimedia services. Iridium and Teledesic have on-board digital processing and switching, while other systems, such as the Globalstar, act as a bent pipe. Despite these differences, from the point of view of providing telephony-based services, the principles of operation are very similar, and thus, the analytical techniques to be developed in the proposed work will be applicable to any LEO satellite system that offers such services.

1.1 Related Research

Despite the importance of satellite systems, their performance has not been adequately evaluated. A typical way of modeling a satellite system in the literature is to represent each cell as an M/M/K/K queue. This approach permits the calculation of various useful performance measures, such as the call blocking probability. However, this type of model does not take into account the fact that the amount of traffic in one cell depends on the amount of traffic in one or more other cells. This type of traffic dependencies are taken into account in our models described in Section 2.

In [6], Ganz *et al.*, investigated the distribution of the number of hand-offs and the average call drop probability for LEO satellite systems. Both beam-to-beam and satellite-to-satellite hand-offs were taken into account. Each cell was modeled as an M/M/K/K queue, where K denotes the number of channels per cell, assuming that the number of hand-off calls entering a cell is equal to the number of hand-off calls leaving the cell. In [8], Jamalipour *et al.*, investigated the traffic characteristics of LEO systems and proposed

a probability density function to locate the position of each user. Using this function, the normalized throughput and average delay was calculated. See also [9, 7]. In [12], Pennoni and Ferroni described an algorithm to improve the performance of LEO systems. They defined two queues for each cell, one for new calls and one for hand-off calls. The calls are held in these two queues for a maximum allowed waiting time. That is, they are dropped if they are not served within this time. The queue for new calls has a maximum waiting time equal to 20 sec. The queue for hand-off calls has a maximum waiting time equal to the cross-over time of the overlapping zone of two adjacent cells. The hand-off queue has higher priority than the new calls queue. Simulation results showed that this algorithm decreased the call dropping rate drastically. In [14], Ruiz *et al.*, used teletraffic techniques to calculate the blocking and hand-off probabilities. Various channel assignment strategies were investigated. In [5], Dosiere *et al.*, defined a model for calculating the hand-off traffic rate. The authors divided a street of coverage into small pieces where each piece is equal to the footprint area of a satellite. Given the total arrival distribution for the whole street of coverage, the arrival rate of each satellite was obtained by integrating that distribution for the satellite interval. The hand-off rate was then calculated through a second integration. Once the hand-off rate has been obtained, the blocking probability can be calculated using the Erlang loss formula.

A number of authors have also dealt with the very interesting problem of routing in a satellite system. In [18, 19], Werner *et al.*, proposed a dynamic routing algorithm for ATM-based LEO and MEO satellite systems. Due to the fact that satellites move in orbits and orbits slowly rotate around the earth, the network topology can be seen as consisting of a series of topologies which continuously repeat themselves. For each topology, end-to-end routes are calculated. Subsequently, an optimization procedure is carried out over all the network topologies with a view to minimizing the occurrence of hand-offs between successive topologies. In [11], Mauger and Rosenberg proposed the *virtual node* routing algorithm for ATM traffic. Users are mapped onto virtual nodes, and each virtual node is served by a satellite. When the satellite passes, the next satellite takes its place and serves the virtual node. Routing is performed according to the topology of the virtual nodes.

Chang *et al.*, proposed the finite state automaton (FSA) model in [3, 1] to solve the ISL link assignment problem in LEO satellite systems. The total time it takes the position of all the satellites over the earth to repeat itself, is divided into equal length intervals during which the visibility between satellites, that is the network topology of the satellites, does not change. Given a traffic matrix for each interval, a link assignment algorithm is run with a view to maximizing the residual capacity of the bottleneck links. The result is a table that shows connectivity between satellites for each interval. These tables can be stored in each satellite, and during the real-time operation of the system the inter-satellite links are established according to these tables. Further related research can be found in [4, 2].

Uzunalioglu *et al.*, suggested in [16, 17] a connection hand-off protocol for LEO satellite systems. First, a minimum cost route for a connection between two points on the earth is obtained. This route is used for as long as possible. When a hand-off occurs at either end of the connection, the protocol simply adds the new link to the path. This continues for a predetermined amount of time, when the protocol computes a new end-to-end path for the connection. In [15], Uzunalioglu proposed a probabilistic routing protocol based on

the above approach. Finally, a new traffic load balancing algorithm was proposed by Kim *et al.*, in [10].

1.2 Contributions and Organization

In this paper we study the problem of carrying voice calls over a LEO satellite network and we present an analytical model for computing call blocking probabilities for a single orbit of a satellite constellation. We first derive an exact Markov process, and corresponding queueing network, for a single orbit under the assumption that satellites are fixed in the sky (i.e., there are no hand-offs of voice calls). We show that the queueing network has a product-form solution, and we develop a method for computing the normalizing constant. In terms of time complexity, our method represents a significant improvement (which we quantify) over a brute-force calculation, however, it can be applied directly to orbits with at most five satellites. For a system with a larger number of satellites, we then present an approximate decomposition algorithm to compute call blocking probabilities by decomposing the system into smaller sub-systems, and solving each sub-system in isolation using the exact solution described above. This approach leads to an iterative scheme, where the individual sub-systems are solved successively until a convergence criterion is satisfied.

Next, we introduce hand-offs by considering the system of satellites as they orbit the earth. For an orbit with earth-fixed coverage, we then show that there is no blocking due to hand-offs, and thus, the solution (exact or approximate) obtained under the assumption that satellites are fixed in the sky can be used to compute call blocking probabilities in this case. For an orbit with satellite-fixed coverage, on the other hand, blocking due to hand-offs does occur. In this case, we show how the queueing network described above can be extended to model call hand-offs by allowing customers to move from one node to another, and we derive the rate of such node-to-node transitions in terms of the speed of the satellites and the shape of the footprints. We also show that the new queueing network has a product-form solution similar to the one under the no-hand-offs assumption, and thus, the exact and approximate algorithms developed above can be applied directly to compute call blocking probabilities under the presence of hand-offs.

The paper is organized as follows. In Section 2 we develop an exact Markov process model under the assumption that satellites are fixed in the sky (i.e., no hand-offs take place), and in Section 3 we present an approximate decomposition algorithm for a large number of satellites. In Section 4 we extend our approach to model hand-offs for both earth-fixed and satellite-fixed coverage. We present numerical results in Section 5, and in Section 6 we conclude the paper by discussing possible directions to which this work may be extended in the future.

2 An Exact Model for the No Hand-Offs Case

Let us first consider the case where the position of the satellites in the single orbit is fixed in the sky, as in the case of geo-stationary satellites. The analysis of such a system is simpler, since no calls are lost due to hand-offs from one satellite to another, as when the satellites move with respect to the users on the earth. This model will be extended in the following section to account for hand-offs in constellations with both

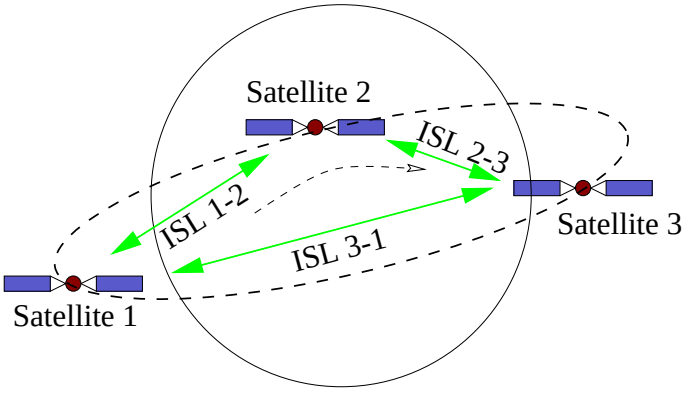

Figure 1: Three satellites in a single orbit

earth-fixed and satellite-fixed coverage.

Each up-and-down link of a satellite has capacity to support up to C_{UDL} calls, while each inter-satellite link has capacity equal to C_{ISL} calls. Let us assume that call requests arrive at each satellite according to a Poisson process, and that call holding times are exponentially distributed. We now show how to compute blocking probabilities for the 3 satellites in the single orbit of Figure 1. The analysis can be generalized to analyze $k > 3$ satellites in a single orbit. For simplicity, we consider only shortest-path routing, although the analysis can be applied to any fixed routing scheme whereby the path taken by a call is fixed and known in advance of the arrival of the call request.

Let n_{ij} be a random variable representing the number of active calls between satellite i and satellite j, $1 \leq i, j \leq 3$, regardless of whether the calls originated at satellite i or j. Let λ_{ij} (respectively, $1/\mu_{ij}$) denote the arrival rate (resp., mean holding time) of calls between satellites i and j. Then, the evolution of the three-satellite system in Figure 1 can be described by the six-dimensional Markov process:

$$\underline{n} \quad = \quad (n_{11}, n_{12}, n_{13}, n_{22}, n_{23}, n_{33}) \tag{1}$$

Also let $\underline{1}_{ij}$ denote a vector with zeros for all random variables except random variable n_{ij} which is 1. The state transition rates for this Markov process are given by:

$$r(\underline{n}, \underline{n} + \underline{1}_{ij}) \quad = \quad \lambda_{ij} \quad \forall\ i, j \tag{2}$$

$$r(\underline{n}, \underline{n} - \underline{1}_{ij}) \quad = \quad n_{ij}\ \mu_{ij} \quad \forall\ i, j,\ n_{ij} > 0 \tag{3}$$

The transition in (2) is due to the arrival of a call between satellites i and j, while the transition in (3) is due to the termination of a call between satellites i and j.

Due to the fact that some of the calls share common up-and-down and inter-satellite links, the following constraints are imposed on the state space:

$$2n_{11} + n_{12} + n_{13} \quad \leq \quad C_{UDL} \tag{4}$$

$$n_{12} + 2n_{22} + n_{23} \quad \leq \quad C_{UDL} \tag{5}$$

$$n_{13} + n_{23} + 2n_{33} \leq C_{UDL} \quad (6)$$

$$n_{12} \leq C_{ISL} \quad (7)$$

$$n_{13} \leq C_{ISL} \quad (8)$$

$$n_{23} \leq C_{ISL} \quad (9)$$

Constraint (4) ensures that the number of calls originating (equivalently, terminating) at satellite 1 is at most equal to the capacity of the up-and-down link of that satellite. Note that a call that originates and terminates within the footprint of satellite 1 captures two channels, thus the term $2n_{11}$ in constraint (4). Constraints (5) and (6) are similar to (4), but correspond to satellites 2 and 3, respectively. Finally, constraints (7)-(9) ensure that the number of calls using the link between two satellites is at most equal to the capacity of that link. Note that, because of (4)-(6), constraints (7)-(9) become redundant when $C_{ISL} \geq C_{UDL}$. In other words, there is no blocking at the inter-satellite links when the capacity of the links is at least equal to the capacity of the up-and-down links at each satellite [1].

It is straightforward to verify that the Markov process for the three-satellite system shown in Figure 1 has a closed-form solution which is given by:

$$P(\underline{n}) = P(n_{11}, n_{12}, n_{13}, n_{22}, n_{23}, n_{33}) = \frac{1}{G} \frac{\rho_{11}^{n_{11}}}{n_{11}!} \frac{\rho_{12}^{n_{12}}}{n_{12}!} \frac{\rho_{13}^{n_{13}}}{n_{13}!} \frac{\rho_{22}^{n_{22}}}{n_{22}!} \frac{\rho_{23}^{n_{23}}}{n_{23}!} \frac{\rho_{33}^{n_{33}}}{n_{33}!} \quad (10)$$

where G is the normalizing constant and $\rho_{ij} = \lambda_{ij}/\mu_{ij},\ i, j = 1, 2, 3$, is the offered load of calls from satellite i to satellite j. As we can see, the solution is the product of six terms of the form $\rho_{ij}^{n_{ij}}/n_{ij}!,\ i, j = 1, 2, 3$, each corresponding to one of the six different types of calls. Therefore, it is easily generalizable to a k-satellite system, $k > 3$.

An alternative way is to regard this Markov process as describing a network of six M/M/K/K queues, one for each type of calls between the three satellites. Since the satellites do not move, there are no hand-offs, and as a consequence customers do not move from one queue to another (we will see in Section 4.2 that hand-offs may be modeled by allowing customers to move between the queues). Now, the probability that there are n customers in an M/M/K/K queue is given by the familiar expression $(\rho^n/n!)/\left(\sum_{k=0}^{K} \rho^k/k!\right)$, and therefore, the probability that there are $(n_{11}, n_{12}, n_{13}, n_{22}, n_{23}, n_{33})$ customers in the six queues is given by (10). Unlike previous studies reported in the literature, our model takes into account the fact that the six M/M/K/K queues are not independent, since the number of customers accepted in each M/M/K/K queue depends on the number of customers in other queues, as described by the constraints (4)-(9).

Of course, the main concern in any product-form solution is the computation of the normalizing constant:

$$G = \sum_{\underline{n}} \frac{\rho_{11}^{n_{11}}}{n_{11}!} \frac{\rho_{12}^{n_{12}}}{n_{12}!} \frac{\rho_{13}^{n_{13}}}{n_{13}!} \frac{\rho_{22}^{n_{22}}}{n_{22}!} \frac{\rho_{23}^{n_{23}}}{n_{23}!} \frac{\rho_{33}^{n_{33}}}{n_{33}!} \quad (11)$$

[1] When there are more than three satellites in an orbit, calls between a number of satellite pairs may share a given inter-satellite link. Consequently, the constraints of a k-satellite orbit, $k > 3$, corresponding to (7)-(9) will be similar to constraints (4)-(6), in that the left-hand side will involve a summation over a number of calls. In this case, blocking on inter-satellite links may occur even if $C_{ISL} \geq C_{UDL}$.

where the sum is taken over all vectors $\underline{n}$ that satisfy constraints (4) through (9). We now show how to compute the normalizing constant G in an efficient manner.

We can write $P(\underline{n})$ as:

$$\begin{aligned} P(n_{11}, n_{12}, n_{13}, n_{22}, n_{23}, n_{33}) &= P(n_{11}, n_{22}, n_{33} \mid n_{12}, n_{13}, n_{23}) P(n_{12}, n_{13}, n_{23}) \\ &= P(n_{11} \mid n_{12}, n_{13}, n_{23})\ P(n_{22} \mid n_{12}, n_{13}, n_{23})\ P(n_{33} \mid n_{12}, n_{13}, n_{23})\ P(n_{12}, n_{13}, n_{23}) \\ &= P(n_{11} \mid n_{12}, n_{13})\ P(n_{22} \mid n_{12}, n_{23})\ P(n_{33} \mid n_{13}, n_{23})\ P(n_{12}, n_{13}, n_{23}) \end{aligned} \tag{12}$$

The second step in expression (12) is due to the fact that, once the values of random variables n_{12}, n_{13}, n_{23}, representing the number of calls in each of the inter-satellite links, is fixed, then the random variables n_{11}, n_{22}, and n_{33} are independent of each other (refer also to Figure 1). The third step in (12) is due to the fact that random variable n_{11} depends on n_{12} and n_{13}, and it is independent of the random variable n_{23}; similarly for random variables n_{22} and n_{33}.

When we fix the values of the random variables n_{12} and n_{13}, the number of up-and-down calls in satellite 1 is described by an M/M/K/K loss system, and thus:

$$P(n_{11} \mid n_{12}, n_{13}) = \sum_{0 \le 2n_{11} \le C_{UDL} - n_{12} - n_{13}} \frac{\rho_{11}^{n_{11}}}{n_{11}!} \tag{13}$$

Similar expressions can be obtained for $P(n_{22} \mid n_{12}, n_{23})$ and $P(n_{33} \mid n_{13}, n_{23})$, corresponding to satellites 2 and 3, respectively. We can now rewrite expression (11) for the normalizing constant as follows:

$$\begin{aligned} G = \sum_{0 \le n_{12}, n_{13}, n_{23} \le \min\{C_{UDL}, C_{ISL}\}} \frac{\rho_{12}^{n_{12}} \rho_{13}^{n_{13}} \rho_{23}^{n_{23}}}{n_{12}! n_{13}! n_{23}!} \Bigg[\left(\sum_{0 \le 2n_{11} \le C_{UDL} - n_{12} - n_{13}} \frac{\rho_{11}^{n_{11}}}{n_{11}!} \right) \\ \times \left(\sum_{0 \le 2n_{22} \le C_{UDL} - n_{12} - n_{23}} \frac{\rho_{22}^{n_{22}}}{n_{22}!} \right) \left(\sum_{0 \le 2n_{33} \le C_{UDL} - n_{13} - n_{23}} \frac{\rho_{33}^{n_{33}}}{n_{33}!} \right) \Bigg] \end{aligned} \tag{14}$$

Let $C = \max\{C_{ISL}, C_{UDL}\}$. Using expression (14) we can see that the normalizing constant can be computed in $O(C^3)$ time rather than the $O(C^6)$ time required by a brute force enumeration of all states, a significant improvement in efficiency.

Once the value of the normalizing constant is obtained, we can compute blocking probabilities by summing up all the appropriate blocking states. Consider the 3-satellite orbit of Figure 1. The probability that a call which either originates or terminates at satellite 1 will be blocked on the up-and-down link of that satellite is given by:

$$P_{UDL_1} = \sum_{2n_{11} + n_{12} + n_{13} = C_{UDL}} P(\underline{n}) \tag{15}$$

while the probability that a call originating at satellite i (or satellite j) and terminating at satellite j (or i) will be blocked by the inter-satellite link (i, j) is:

$$P_{ISL_{ij}} = \begin{cases} 0, & C_{ISL} > C_{UDL} \\ \sum_{n_{ij}=C_{ISL}} P(\underline{n}), & \text{otherwise} \end{cases} \quad (16)$$

Once the blocking probabilities on all up-and-down and inter-satellite links have been obtained using expressions similar to (15) and (16), the blocking probability of calls between any two satellites can be easily obtained. We note that expressions (15) and (16) explicitly enumerate all relevant blocking states, and thus, they involve summations over appropriate parts of the state space of the Markov process for the satellite orbit. Consequently, direct computation of the link blocking probabilities using these expressions can be computationally expensive. We have been able to express the up-and-down and inter-satellite link blocking probabilities in a way that allows us to compute these probabilities as a byproduct of the computation of the normalizing G. As a result, all blocking probabilities in a satellite orbit can be computed in an amount of time that is equal to the time needed to obtain the normalizing constant, plus a constant. The derivation of the expressions for the link blocking probabilities is a straightforward generalization of the technique employed in (12) and is omitted.

3 A Decomposition Algorithm for the No Hand-Offs Case

Let k be the number of satellites in a single orbit, and N be the number of random variables in the state description of the corresponding Markov process, $N = k(k+1)/2$. Using the method described above, we can compute the normalizing constant G in time $O(C^{N-k})$ as opposed to time $O(C^N)$ needed by a brute force enumeration of all states. Although the *improvement* in the running time provided by our method for computing G increases with k, the value of N will dominate for large values of k. Numerical experiments with the above algorithm indicate that this method is limited to $k = 5$ satellites. That is, it takes an amount of time in the order of a few minutes to compute the normalizing constant G for 5 satellites. Thus, a different method is needed for analyzing realistic constellations of LEO satellites.

In this section we present a method to analyze a single orbit with k satellites, $k > 5$, by decomposing the orbit into sub-systems of 3 or fewer satellites. Each sub-system is analyzed separately, and the results obtained by the sub-systems are combined using an iterative scheme.

In order to explain how the decomposition algorithm works, let us consider the case of a six-satellite orbit, as shown in Figure 2(a). This orbit is divided into two sub-systems. Sub-system 1 consists of satellites 1, 2, and 3, and sub-system 2 consists of satellites 4, 5, and 6. In order to analyze sub-system 1 in isolation, we need to have some information from sub-system 2. Specifically, we need to know the probability that a call originating at a satellite in sub-system 1 and terminating at a satellite in sub-system 2 will be blocked due to lack of capacity in a link in sub-system 2. Also, we need to know the number of calls originating from sub-system 2 and terminating in sub-system 1. Similar information is needed from sub-system 1, in order to analyze sub-system 2.

In view of this, each sub-system is augmented to include two fictitious satellites which represent the aggregate behavior of the other sub-system. In sub-system 1, we add two new satellites, which we call N1

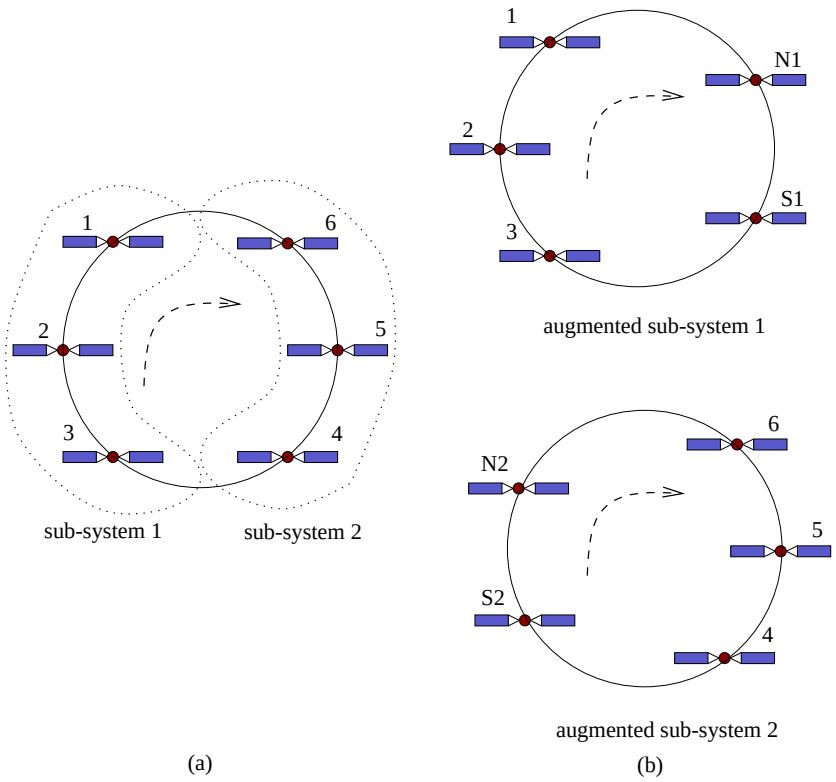

Figure 2: (a) Original 6-satellite orbit, (b) augmented sub-systems

and S1, as shown in Figure 2(b). A call originating at a satellite $i, i = 1, 2, 3$, and terminating at a satellite $j, j = 4, 5, 6$, will be represented by a call from i to one of the fictitious satellites (N1 or S1). Depending upon i and j, this call may be routed differently. For instance, let us assume that $i = 2$ and $j = 4$. Then, in our augmented sub-system 1, this call will be routed to satellite S1 through satellite 3. However, if $j = 6$, the call will be routed to satellite N1 through satellite 1 [2]. In other words, satellite N1 (respectively, S1) in the augmented sub-system 1 is the destination for calls of the original orbit that originate from satellite $i, i = 1, 2, 3$ and are routed to satellite $j, j = 4, 5, 6$ in the clockwise (respectively, counter-clockwise) direction in Figure 2(a). Similarly, calls originating from satellite $j, j = 4, 5, 6$, to satellite $i, i = 1, 2, 3$, and are routed in the counter-clockwise (respectively, clockwise) direction, are represented in sub-system 1 as calls originating from N1 (respectively, S1) to i. Again, the originating satellite (N1 or S1) for the call depends on the values of i and j and the path the call follows in the original 6-satellite orbit.

Sub-system 2 is likewise augmented to include two fictitious satellites, N2 and S2 (see Figure 2(b)), which represent the aggregate behavior of sub-system 1. Satellites N2 and S2 become the origin and destination of calls traveling from sub-system 2 to sub-system 1, and vice versa, in a manner similar to N1 and S1 described above.

A summary of our iterative algorithm is provided in Figure 3. Below we describe the decomposition

[2] While this discussion assumes shortest-path routing, our model can handle any fixed-routing scheme.

Decomposition Algorithm for A Single Orbit

A 6-satellite orbit is decomposed into two 3-satellite sub-systems as in Figure 2. Sub-system 1 consists of satellites 1 to 3 in the original orbit plus fictitious satellites N1 and S1, while sub-system 2 consists of satellites 4 to 6 of the original orbit plus fictitious satellites N2 and S2.

1. begin
2. $h \leftarrow 0$ //Initialization step
   // $p_{ij}(h)$ is the probability that an inter-sub-system call will be blocked in sub-system 1
   // $q_{ij}(h)$ is the probability that an inter-sub-system call will be blocked in sub-system 2
   $q_{ij}(h) \leftarrow 0, \quad 1 \leq i \leq 3 < j \leq 6$
3. $h \leftarrow h + 1$ //h-th iteration
4. $\lambda_{ij}(h) \leftarrow \lambda_{ij}, \quad 1 \leq i \leq j \leq 3$ //Sub-system 1
   $\lambda_{1,N1} = (1 - q_{16})\lambda_{16} + (1 - q_{15})\lambda_{15}$
   $\lambda_{1,S1} = (1 - q_{14})\lambda_{14}$
   $\lambda_{2,N1} = (1 - q_{26})\lambda_{26} + (1 - q_{25})\lambda_{25}$
   $\lambda_{2,S1} = (1 - q_{24})\lambda_{24}$
   $\lambda_{3,N1} = (1 - q_{36})\lambda_{36}$
   $\lambda_{3,S1} = (1 - q_{34})\lambda_{34} + (1 - q_{35})\lambda_{35}$
   Solve sub-system 1 to obtain new values for $p_{ij}(h)$
5. $\lambda_{ij}(h) \leftarrow \lambda_{ij}, \quad 4 \leq i \leq j \leq 6$ //Sub-system 2
   $\lambda_{N2,4} = 0$
   $\lambda_{S2,4} = (1 - p_{14})\lambda_{14} + (1 - p_{24})\lambda_{24} + (1 - p_{34})\lambda_{34}$
   $\lambda_{N2,5} = (1 - p_{15})\lambda_{15} + (1 - p_{25})\lambda_{25}$
   $\lambda_{S2,5} = (1 - p_{35})\lambda_{35}$
   $\lambda_{N2,6} = (1 - p_{16})\lambda_{16} + (1 - p_{26})\lambda_{26} + (1 - p_{36})\lambda_{36}$
   $\lambda_{S2,6} = 0$
   Solve sub-system 2 to obtain new values for $p_{ij}(h)$
6. Repeat from Step 3 until the blocking probabilities converge
7. end of the algorithm

Figure 3: Decomposition algorithm for a single orbit of a satellite constellation

algorithm using the 6-satellite orbit shown in Figure 2(a). Recall that $\lambda_{ij}, 1 \leq i \leq j$, is the arrival rate of calls between satellites i and j. For analyzing the augmented sub-systems in Figure 2(b), we will introduce the new arrival rates $\lambda_{i,N1}$, $\lambda_{i,S1}$, $\lambda_{N2,j}$, and $\lambda_{S2,j}$, $i = 1, 2, 3$, $j = 4, 5, 6$. Specifically, $\lambda_{i,N1}$ (respectively, $\lambda_{i,S1}$) accounts for all calls between satellite $i, i = 1, 2, 3$, and a satellite in sub-system 2 that are routed in the clockwise (respectively, counter-clockwise) direction. Similarly, $\lambda_{N2,j}$ (respectively, $\lambda_{S2,j}$) accounts for all calls between sub-system 1 and satellite $j, j = 4, 5, 6$ that are routed in the clockwise (respectively, counter-clockwise) direction.

Initially, we solve sub-system 1 in isolation using:

$$\lambda_{1,N1} = (1 - q_{16})\lambda_{16} + (1 - q_{15})\lambda_{15} \tag{17}$$

$$\lambda_{1,S1} = (1 - q_{14})\lambda_{14} \tag{18}$$

$$\lambda_{2,N1} = (1 - q_{26})\lambda_{26} + (1 - q_{25})\lambda_{25} \tag{19}$$

$$\lambda_{2,S1} = (1 - q_{24})\lambda_{24} \tag{20}$$

$$\lambda_{3,N1} = (1 - q_{36})\lambda_{36} \tag{21}$$

$$\lambda_{3,S1} = (1 - q_{34})\lambda_{34} + (1 - q_{35})\lambda_{35} \tag{22}$$

Quantity $q_{ij}, 1 \leq i \leq 3 < j \leq 6$, represents the current estimate of the probability that a call between a satellite i in sub-system 1 and and satellite j in sub-system 2 will be blocked due to lack of capacity in a link of sub-system 2. For the first iteration, we use $q_{ij} = 0$ for all i and j; how these values are updated in subsequent iterations will be described shortly. Thus, the term $(1 - q_{16})\lambda_{16}$ in (17) represents the *effective* arrival rate of calls between satellites 1 and 6, as seen by sub-system 1; similarly for the other terms in (17)–(22).

The solution to the first sub-system yields an initial value for the probability $p_{ij}, 1 \leq i \leq 3 < j \leq 6$, that a call between a satellite i in sub-system 1 and a satellite j in sub-system 2 will be blocked due to lack of capacity in a link of sub-system 1. Therefore, the effective arrival rates of calls between, say, satellite 1 and satellite 4, that is offered to sub-system 2 can be initially estimated as $(1 - p_{16})\lambda_{16}$. We can now solve sub-system 2 in isolation using [3]:

$$\lambda_{N2,4} = 0 \tag{23}$$

$$\lambda_{S2,4} = (1 - p_{14})\lambda_{14} + (1 - p_{24})\lambda_{24} + (1 - p_{34})\lambda_{34} \tag{24}$$

$$\lambda_{N2,5} = (1 - p_{15})\lambda_{15} + (1 - p_{25})\lambda_{25} \tag{25}$$

$$\lambda_{S2,5} = (1 - p_{35})\lambda_{35} \tag{26}$$

$$\lambda_{N2,6} = (1 - p_{16})\lambda_{16} + (1 - p_{26})\lambda_{26} + (1 - p_{36})\lambda_{36} \tag{27}$$

$$\lambda_{S2,6} = 0 \tag{28}$$

[3] In (23) we have that $\lambda_{N2,4} = 0$ because we assume that calls between satellites in sub-system 1 and satellite 4 are routed in the counter-clockwise direction; similarly for expression (28).

Based on the above discussion, $\lambda_{S2,4}$ in (24) represents the effective arrival rate of calls between a satellite in sub-system 1 and satellite 4, as seen by sub-system 2. Expressions (23)–(28) can be explained in a similar manner. The solution to the second sub-system provides an estimate of the blocking probabilities $q_{ij}, 1 \leq i \leq 3 < j \leq 6$, that calls between satellites in the two sub-systems will be blocked due to lack of capacity in a link of sub-system 2.

The new estimates for q_{ij} are then used in expressions (17) to (22) to update the arrival rates to the two fictitious satellites of augmented sub-system 1. Sub-system 1 is then solved again, and the estimates p_{ij} are updated and used in expressions (23) to (28) to obtain new arrival rates for the fictitious satellites of sub-system 2. This leads to an iterative scheme, where the two sub-systems are solved successively until a convergence criterion (e.g., in terms of the values of the call blocking probabilities) is satisfied.

Orbits consisting of any number $k > 5$ of satellites can be decomposed into a number of sub-systems, each consisting of 3 satellites of the original orbit (the last sub-system may consist of fewer than 3 satellites). The decomposition method is similar to the one above, in that for sub-system l, the remaining satellites are aggregated to two fictitious satellites. Each sub-system is analyzed in succession as described above. The decomposition algorithm described above is similar in spirit to the decomposition algorithms developed for tandem queueing networks with finite capacity queues (see [13]). We note that when employing the decomposition algorithm, the selection of the sub-system size will depend on the number of satellites in the original orbit and how efficiently we can calculate the exact solution of the Markov process associated with each sub-system. It is well known in decomposition algorithms that the larger the individual sub-systems that have to be analyzed in isolation, the better the accuracy of the decomposition algorithm. Thus, as we mentioned above, we have decided to decompose an orbit into sub-systems of the largest size (three of the original satellites plus two fictitious ones) for which we can efficiently analyze the Markov process, plus, possibly, a sub-system of smaller size, if the number of satellites is not a multiple of three.

4 Modeling Hand-Offs

4.1 Earth-Fixed Coverage

Let us now turn to the problem of determining blocking probabilities in a single orbit of satellites with earth-fixed coverage. Let k denote the number of satellites in the orbit. In this case we assume that the earth is divided into k fixed cells (footprints) and that time is divided in intervals of length T such that, during a given interval, each satellite serves a certain cell by continuously redirecting its beams. At the end of each interval, i.e., every T time units, all satellites simultaneously redirect their beams to serve the next footprint along their orbit, and they also hand-off currently served calls to the next satellite in the orbit.

We make the following observations about this system. Hand-off events are periodic with a period of T time units, and hand-offs take place in bulk at the end of each period. Also, there is no call blocking due to hand-offs, since, at each hand-off event a satellite passes its calls to the one following it and simply inherits the calls of the satellite ahead of it. Finally, within each period T, the system can be modeled as one with no

hand-offs, such as the one described in the previous subsection. Given that the period T is equal to the orbit period (approximately 90 minutes) divided by the number of satellites (e.g., 11 for the Iridium constellation) we can assume that the system reaches steady state within the period, and thus, the initial conditions (i.e., the number of calls inherited by each satellite at the beginning of the period) do not affect its behavior.

Now, since every T units of time, each satellite assumes the traffic carried by the satellite ahead, from the point of view of an observer on the earth, this system appears to be as if the satellites are permanently fixed over their footprints. Hence, we can use the decomposition algorithm presented above to analyze this system.

4.2 Satellite-Fixed Coverage

Consider now satellite-fixed cell coverage. As a satellite moves, its footprint on the earth (the cell served by the satellite) also moves with it. As customers move out of the footprint area of a satellite, their calls are handed off to the satellite following it from behind. In order to model hand-offs in this case, we make the assumption that potential customers are uniformly distributed over the part of the earth served by the satellites in the orbit. This assumption has the following two consequences.

- The arrival rate λ to each satellite remains constant as it moves around the earth. Then, the arrival rate of calls between satellite i and satellite j is given by $\lambda_{ij} = \lambda r_{ij}$, where r_{ij} is the probability that a call originating by a customer served by satellite i is for a customer served by satellite j.
- The active customers served by a satellite can be assumed to be uniformly distributed over the satellite's footprint. As a result, the rate of hand-offs from satellite i to satellite j that is following from behind is proportional to the number of calls at satellite i.

Clearly, the assumption that customers are uniformly distributed (even within an orbit) is an approximation. In Section 6 we will discuss how we are currently extending the results presented in this section to accurately model the situation when customers are not uniformly distributed.

Let A denote the area of a satellite's footprint and v denote a satellite's speed. As a satellite moves around the earth, within a time interval of length Δt, its footprint will move a distance of ΔL, as shown in Figure 4. Calls involving customers located in the part of the original footprint of area ΔA (the hand-off area) that is no longer served by the satellite are handed off to the satellite following it. Let $\Delta A = A\beta\Delta L$, where β depends on the shape of the footprint. Because of the assumption that active customers are uniformly distributed over the satellite's footprint, the probability q that a customer will be handed off to the next satellite along the sky within a time interval of length Δt is

$$q = \frac{\Delta A}{A} = \beta\Delta L = \beta v\Delta t \tag{29}$$

Define $\alpha = \beta v$. Then, when there are n customers served by a satellite, the *rate* of hand-offs to the satellite following it will be αn.

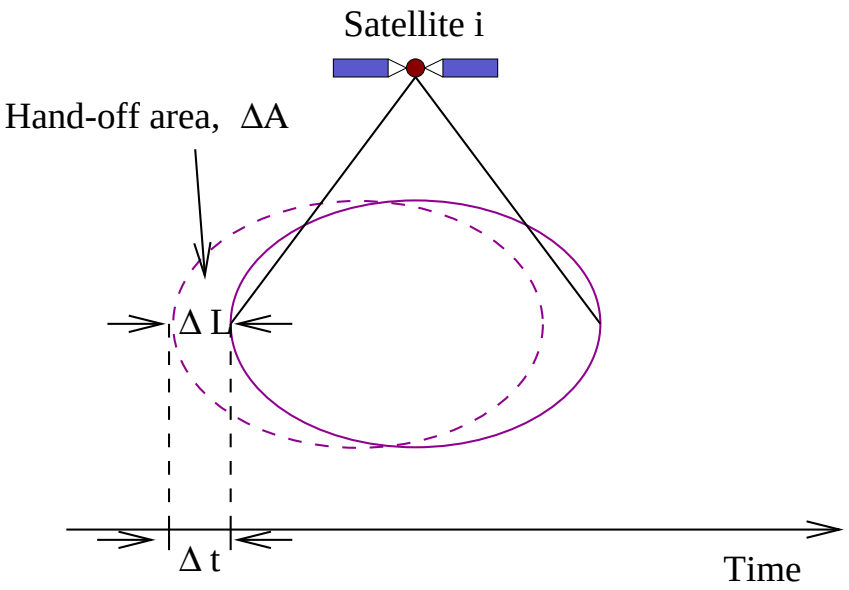

Figure 4: Calculation of the hand-off probability

Let us now return to the 3-satellite orbit (see Figure 1) and introduce hand-offs. This system can be described by a continuous-time Markov process with the same number of random variables as the no-hand-offs model of Section 2 (i.e., $n_{11}, \cdots, n_{33}$), the same transition rates (2) and (3), but with a number of additional transition rates to account for hand-offs. We will now derive the transition rates due to hand-offs.

Consider calls between a customer served by satellite 1 and a customer served by satellite 2. There are n_{12} such calls serving $2n_{12}$ customers: n_{12} customers on the footprint of satellite 1 and n_{12} on the footprint of satellite 2. Consider a call between customer A and customer B, served by satellite 1 and 2, respectively. The probability that customer A will be in the hand-off area of satellite 1 but B will not be in the hand-off area of satellite 2 is $q(1-q) = q - q^2$. But, from (29), we have that $\lim_{\Delta t \to 0} \frac{q^2}{\Delta t} = 0$, so the rate at which these calls experience a hand-off from satellite 1 to satellite 3 that follows it is αn_{12}. Let $\underline{n} = (n_{11}, n_{12}, n_{13}, n_{22}, n_{23}, n_{33})$, and define $\underline{1}_{ij}$ as a vector of zeroes for all variables except variable n_{ij} which is 1. Based on the above discussion, we thus have:

$$r(\underline{n}, \underline{n} - \underline{1}_{12} + \underline{1}_{23}) \quad = \quad \alpha n_{12}, \quad n_{12} > 0 \tag{30}$$

Similarly, the probability that customer B will be in the hand-off area of satellite 2 but A will not be in the hand-off area of satellite 1 is $q(1-q) = q - q^2$. Thus, the rate at which these calls experience a hand-off from satellite 2 to satellite 1 that follows it is again αn_{12}:

$$r(\underline{n}, \underline{n} - \underline{1}_{12} + \underline{1}_{11}) \quad = \quad \alpha n_{12}, \quad n_{12} > 0 \tag{31}$$

On the other hand, the probability that both customers A and B are in the hand-off area of their respective satellites is q^2, which, from (29) is $o(\Delta t)$, and thus simultaneous hand-offs are not allowed.

Now consider calls between customers that are both served by the same satellite, say, satellite 1. There are n_{11} such calls serving $2n_11$ customers. The probability that exactly one of the customers of a call is in the hand-off area of satellite 1 is $2q(1-q)$, so the rate at which these calls experience hand-offs (involving a single customer) to satellite 3 is $2\alpha n_{11}$:

$$r(\underline{n}, \underline{n} - \underline{1}_{11} + \underline{1}_{13}) = 2\alpha n_{11}, \quad n_{11} > 0 \tag{32}$$

As before, the probability that both customers of the call are in the hand-off area of satellite 1 is q^2, and again, no simultaneous hand-offs are allowed.

The transition rates involving the other four random variables in the state description (1) can be derived using similar arguments. For completeness, these transition rates are provided in (33)-(38).

$$r(\underline{n}, \underline{n} - \underline{1}_{13} + \underline{1}_{12}) = \alpha n_{13}, \quad n_{13} > 0 \tag{33}$$

$$r(\underline{n}, \underline{n} - \underline{1}_{13} + \underline{1}_{11}) = \alpha n_{13}, \quad n_{13} > 0 \tag{34}$$

$$r(\underline{n}, \underline{n} - \underline{1}_{22} + \underline{1}_{12}) = 2\alpha n_{22}, \quad n_{22} > 0 \tag{35}$$

$$r(\underline{n}, \underline{n} - \underline{1}_{23} + \underline{1}_{13}) = \alpha n_{23}, \quad n_{23} > 0 \tag{36}$$

$$r(\underline{n}, \underline{n} - \underline{1}_{23} + \underline{1}_{22}) = \alpha n_{23}, \quad n_{23} > 0 \tag{37}$$

$$r(\underline{n}, \underline{n} - \underline{1}_{33} + \underline{1}_{23}) = 2\alpha n_{33}, \quad n_{33} > 0 \tag{38}$$

From the queueing point of view, this system is the queueing network of M/M/K/K queues described in Section 2, where customers are allowed to move between queues according to (30)-(38). (Recall that in the queueing model of Section 2, customers are not allowed to move from node to node.) This queueing network has a product-form solution similar to (10). Let γ_{ij} denote the total arrival rate of calls between satellites i and j, including at a rate of λ_{ij}) and hand-off calls (arriving at an appropriate rate). The values of γ_{ij} can be obtained by solving the traffic equations for the queueing network. Let also $\nu_{ij} n_{ij}$ be the departure rate when there are n_{ij} of these calls, including call termination (at a rate of $\mu_{ij} n_{ij}$) and call hand-off (at a rate of $2\alpha n_{ij}$). Also, define $\rho'_{ij} = \gamma_{ij}/\nu_{ij}$. Then, the solution for this queueing network is given by:

$$P(\underline{n}) = P(n_{11}, n_{12}, n_{13}, n_{22}, n_{23}, n_{33}) = \frac{1}{G} \frac{(\rho'_{11})^{n_{11}}}{n_{11}!} \frac{(\rho'_{12})^{n_{12}}}{n_{12}!} \frac{(\rho'_{13})^{n_{13}}}{n_{13}!} \frac{(\rho'_{22})^{n_{22}}}{n_{22}!} \frac{(\rho'_{23})^{n_{23}}}{n_{23}!} \frac{(\rho'_{33})^{n_{33}}}{n_{33}!} \tag{39}$$

which is identical to (10) except that ρ_{ij} has been replaced by ρ'_{ij}.

The product-form solution (39) can be generalized in a straightforward manner for any k-satellite orbit, $k > 3$. We can thus use the techniques developed in Section 2 to solve the system involving hand-offs exactly, or we can use the decomposition algorithm presented in Section 3 to solve orbits with a large number of satellites.

5 Numerical Results

In this section we validate both the exact model and the decomposition algorithm by comparing to simulation results. In the figures presented, simulation results are plotted along with 95% confidence intervals estimated by the method of replications. The number of replications is 30, with each simulation run lasting until each type of call has at least 15,000 arrivals. For the approximate results, the iterative decomposition algorithm terminates when all call blocking probability values have converged within 10^{-6}.

For the results presented here we consider three different traffic patterns; similar results have been obtained for several other patterns. Let r_{ij} denote the probability that a call originating by a customer served by satellite i is for a customer served by satellite j. The first pattern is a uniform traffic pattern such that:

$$r_{ij} = \frac{1}{k} \ \forall\, i,j \qquad \text{(uniform pattern)} \tag{40}$$

where k is the number of satellites. The second is a pattern based on the assumption of traffic locality. Specifically, it assumes that most calls originating at a satellite i are to users in satellites $i-1$, i, and $i+1$, where addition and subtraction is modulo-k for a k-satellite orbit:

$$r_{ij} = \begin{cases} 0.3, & j = i-1, i, i+1 \\ \frac{0.1}{k-3}, & j \neq i-1, i, i+1 \end{cases} \qquad \text{(locality pattern)} \tag{41}$$

The third pattern is such that there are two communities of users, and most traffic is between users within a given community (e.g., satellites over different hemispheres of the earth):

$$r_{ij} = \begin{cases} \frac{0.8}{k/2}, & i,j = 1,\cdots,k/2, \text{ or } i,j = k/2+1,\cdots,k \qquad (2-\text{community pattern}) \\ \frac{0.2}{k/3}, & i = 1,\cdots,k/2, j = k/2+1,\cdots,k \text{ or } j = 1,\cdots,k/2, i = k/2+1,\cdots,k \end{cases} \tag{42}$$

5.1 Validation of the Exact Model

In this section we validate the exact Markov process model for the no hand-offs case developed in Section 2. Recall that we can directly compute the normalizing constant G using expression (14) for orbits of up to five satellites. Thus, we compare the blocking probability values obtained by solving the exact Markov process to simulation results for a 5-satellite orbit and the three traffic patterns discussed above.

Figure 5 plots the blocking probability against the capacity C_{UDL} of up-and-down links, when the arrival rate $\lambda = 10$ and the capacity of inter-satellite links $C_{ISL} = 10$, for the uniform traffic pattern. Three sets of plots are shown: one for calls originating and terminating at the same satellite (referred to as "local calls" in the figure), one for calls traveling over a single inter-satellite link, and one for calls traveling over two inter-satellite links [4]. Each set consists of two plots, one corresponding to blocking probability values obtained by solving the Markov process, and one corresponding to simulation results.

From the figure, we observe that, as the capacity C_{UDL} of up-and-down links increases, the blocking probability of all calls decreases. However, for calls traveling over at least one inter-satellite link, the

[4] These are the only possible types of calls in a 5-satellite orbit and shortest path routing. Furthermore, because of symmetry, the results are the same regardless of the satellite at which the calls originate or terminate.

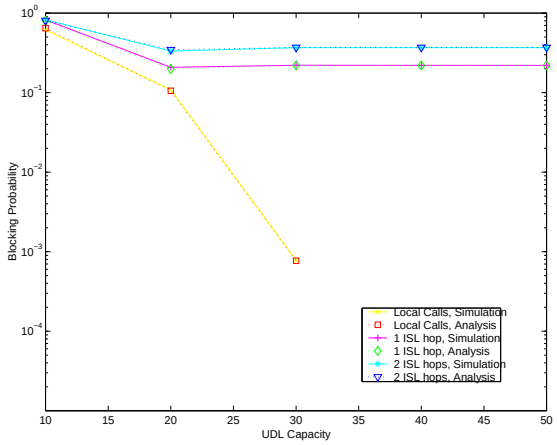

Figure 5: Call blocking probabilities for a 5-satellite orbit, $\lambda = 10$, $C_{ISL} = 10$, uniform pattern

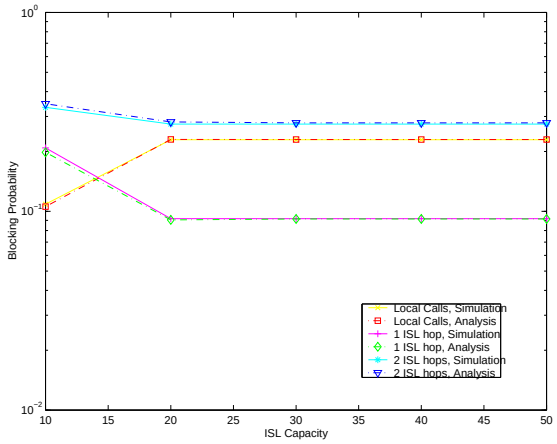

Figure 6: Call blocking probabilities for a 5-satellite orbit, $\lambda = 10$, $C_{UDL} = 20$, uniform pattern

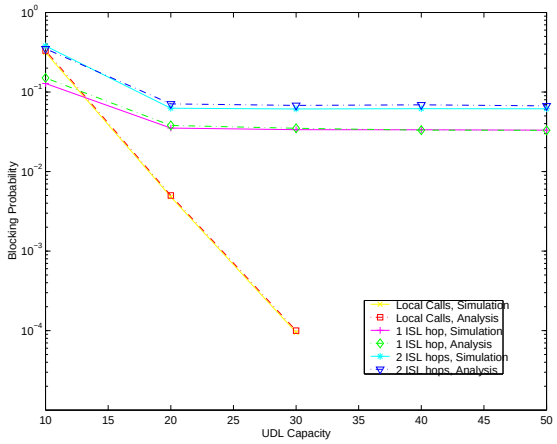

Figure 7: Call blocking probabilities for a 5-satellite orbit, $\lambda = 5$, $C_{ISL} = 10$, uniform pattern

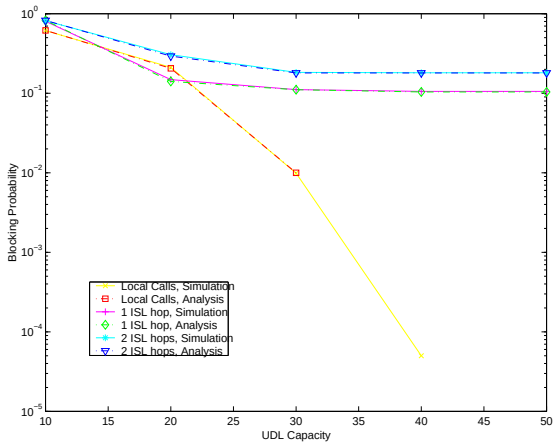

Figure 8: Call blocking probabilities for a 5-satellite orbit, $\lambda = 10$, $C_{ISL} = 10$, locality pattern

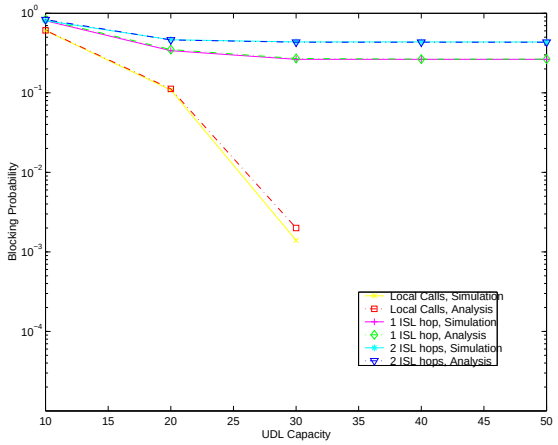

Figure 9: Call blocking probabilities for a 5-satellite orbit, $\lambda = 10$, $C_{ISL} = 10$, 2-community pattern

blocking probability curve flattens out after an initial drop. This behavior is due to the fact that, for small values of C_{UDL}, the up-and-down links represent a bottleneck, thus, increasing C_{UDL} reduces the call blocking probability significantly. However, once C_{UDL} increases beyond a certain value, the inter-satellite links become the bottleneck, and the blocking probability of calls that have to travel over these links is not affected further. On the other hand, the blocking probability of calls not using inter-satellite links (i.e., those originating and terminating at the same satellite) decreases rapidly as C_{UDL} increases, dropping to zero for values $C_{UDL} > 30$ (because of the logarithmic scale, values of zero cannot be shown in Figure 5, so there are no values plotted when $C_{UDL} > 30$ for the curves of local calls).

Figure 6 plots the blocking probability for the same calls as in Figure 5, against the capacity C_{ISL} of inter-satellite links; for the results presented we assume that $\lambda = 10$ and $C_{UDL} = 20$. In this figure we can see that as the value of C_{ISL} increases, the blocking probability of calls using inter-satellite links decreases, as expected. However, the blocking probability of local calls (i.e., calls originating and terminating at the

same satellite which do not use inter-satellite links) increases with increasing C_{ISL}. This behavior can be explained by noting that, as C_{ISL} increases, a larger number of non-local calls (i.e., calls using inter-satellite links) is accepted (since their blocking probability decreases). Since both local and non-local calls compete for up-and-down links, an increase in the number of non-local calls accepted will result in higher blocking probability for local calls. But when the value of C_{ISL} exceeds the value of C_{UDL} (which is equal to 20 in this case), the up-and-down links become the bottleneck, and further increases in C_{ISL} have no effect on blocking probabilities.

Figure 7 is similar to Figure 5 except that the arrival rate is $\lambda = 5$ instead of 10 (all other parameters are as in Figure 5). The behavior of the various curves is similar to that in Figure 5. The main difference is that the blocking probabilities in Figure 7 are significantly lower, a result that is expected due to the lower arrival rate.

Finally, Figures 8 and 9 show results for the same parameters as in Figure 5, but correspond to the locality and 2-community traffic patterns, respectively. Again, the behavior of the curves is similar for all three figures, although the actual blocking probability values depend on the traffic pattern used.

The results in Figures 5–9 illustrate the fact that the blocking probability values obtained by solving the Markov process match the simulation results; this is expected since the Markov process model we developed is exact. Thus, this model can be used to study the interplay between various system parameters (e.g., C_{ISL}, C_{UDL}, traffic pattern, etc.) and their effect on the call blocking probabilities, in an efficient manner. We note that solving the Markov process takes only a few minutes, while running the simulation takes anywhere between 30 minutes and several hours, depending on the value of the arrival rates.

5.2 Validation of the Decomposition Algorithm

We now validate the decomposition algorithm developed in Section 3 by comparing the blocking probabilities obtained by running the algorithm to simulation results. We consider a single orbit of a satellite constellation consisting of 12 satellites, a number representative of typical commercial satellite systems. In all cases studied, we have found that the algorithms converges in only a few (less than ten) iterations, taking a few minutes to terminate. On the other hand, simulation of 12-satellite orbits is quite expensive in terms of computation time, taking several hours to complete.

Figure 10 plots the blocking probability against the capacity C_{UDL} of up-and-down links, when the arrival rate $\lambda = 5$ and the capacity of inter-satellite links $C_{ISL} = 20$, for the uniform traffic pattern. Six sets of calls are shown, one for local calls, and five for non-local calls. Each set consists of two plots, one corresponding to blocking probability values obtained by running the decomposition algorithm of Section 3, and one corresponding to simulation results. Each non-local call for which results are shown travels over a different number of inter-satellite links, from one to five. Thus, the results in Figure 10 represent calls between all the different sub-systems in which the 12-satellite orbit is decomposed by the decomposition algorithm.

From the figure we observe the excellent agreement between the analytical results and simulation. The

behavior of the curves can be explained by noting that, when the capacity C_{UDL} of up-and-down links is less than 20, these links represent a bottleneck. Thus, increasing the up-and-down link capacity results in a significant drop in the blocking probability for all calls. When $C_{UDL} > 20$, however, the inter-satellite links become the bottleneck, and non-local calls do not benefit from further increases in the up-and-down link capacity. We also observe that, the larger the number of inter-satellite links over which a non-local call must travel, the higher its blocking probability, as expected. The blocking probability of local calls, on the other hand, drops to zero for $C_{UDL} > 20$ since they do not have to compete for inter-satellite links.

Figures 11 and 12 are similar to Figure 10 but show results for the locality and 2-community traffic patterns, respectively. For the results presented we used $\lambda = 5$ and $C_{ISL} = 10$, and we varied the value of C_{UDL}. We observe that the values of the call blocking probabilities depend on the actual traffic pattern, but the behavior of the various curves is similar to that in Figure 10. Finally, in Figure 13, we fix the value of C_{UDL} to 20, and we plot the call blocking probabilities for the 2-community traffic pattern against the capacity C_{ISL} of the inter-satellite links.

Overall, the results in Figures 10–13 indicate that analytical results are in good agreement with simulation over a wide range of traffic patterns and system parameters. Thus, our decomposition algorithm can be used to estimate call blocking probabilities in LEO satellite systems in an efficient manner.

6 Concluding Remarks

We have presented an analytical model for computing blocking probabilities for a single orbit of a LEO satellite constellation. We have devised a method for solving the exact Markov process efficiently for up to 5-satellite orbits. For orbits consisting of a larger number of satellites, we have developed an approximate decomposition algorithm to compute the call blocking probabilities by decomposing the system into smaller sub-systems, and iteratively solving each sub-system in isolation using the exact Markov process. We have also shown how our approach can capture blocking due to hand-offs for both satellite-fixed and earth-fixed orbits.

We are currently extending the decomposition algorithm to handle an entire satellite constellation. Assuming that the constellation consists of R orbits, a natural approach is to decompose it into R sub-systems, each representing a single orbit. We are also planning to analyze the case of heterogeneous traffic. One approach to account for different geographic arrival rates, is to segment the band of earth covered by the satellites into fixed regions, each with a different arrival rate of new calls. This approach gives rise to a periodic Markov process model whose special structure can be exploited to solve it efficiently.

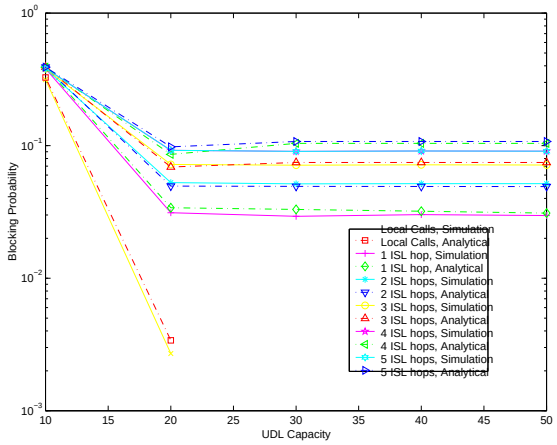

Figure 10: Call blocking probabilities for a 12-satellite orbit, $\lambda = 5$, $C_{ISL} = 20$, uniform pattern

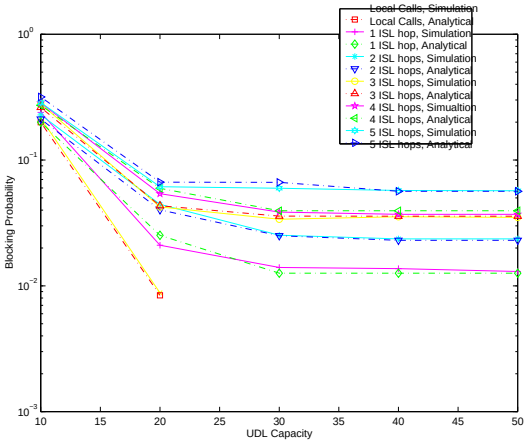

Figure 11: Call blocking probabilities for a 12-satellite orbit, $\lambda = 5$, $C_{ISL} = 10$, locality pattern

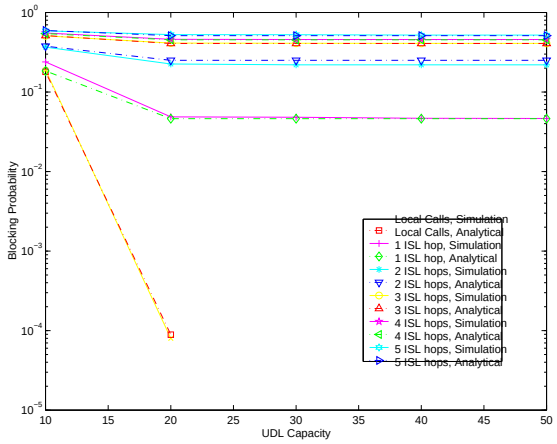

Figure 12: Call blocking probabilities for a 12-satellite orbit, $\lambda = 5$, $C_{ISL} = 10$, 2-community pattern

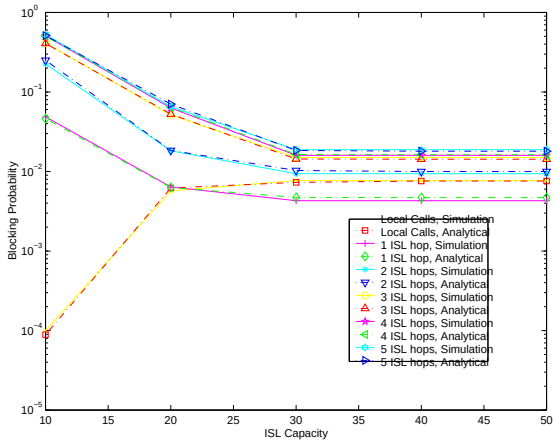

Figure 13: Call blocking probabilities for a 12-satellite orbit, $\lambda = 5$, $C_{UDL} = 20$, 2-community pattern

References

[1] H. S. Chang, B. W. Kim, C. G. Lee, S. L. Min, Y. Choi, H. S. Yang, and C. S. Kim. Topological design and routing for LEO satellite networks. In *IEEE Globecom*, pages 529–535, 1995.

[2] H. S. Chang, B. W. Kim, C. G. Lee, S. L. Min, Y. Choi, H. S. Yang, D. N. Kim, and C. S. Kim. Performance comparison of optimal routing and dynamic routing in low earth orbit satellite networks. In *IEEE Vehicular Technology Conference*, pages 1244–1249, 1996.

[3] H. S. Chang, B. W. Kim, C. G. Lee, S. L. Min, Y. Choi, H. S. Yang, D. N. Kim, and C. S. Kim. Performance comparison of static routing and dynamic routing in low earth orbit satellite networks. In *IEEE Vehicular Technology Conference*, pages 1240–1243, 1996.

[4] H. S. Chang, B. W. Kim, C. G. Lee, S. L. Min, Y. Choi, H. S. Yang, D. N. Kim, and C. S. Kim. FSA-based link assignment and routing in low earth orbit satellite networks. *IEEE Transactions on Vehicular Technology*, 47(3):1037–1048, August 1998.

[5] F. Dosiere, T. Zein, G. Maral, and J. P. Boutes. A model for the handover traffic in low earth-orbiting satellite networks for personal communications. In *IEEE Globecom*, 1993.

[6] A. Ganz, Y. Gong, and B. Li. Performance study of low earth orbit satellite systems. *IEEE Transactions on Communications*, 42(2/3/4), February/March/April 1994.

[7] A. Jamalipour. *Low Earth Orbital Satellites for Personal Communication Networks.* Artech House Publishers, MA, 1998.

[8] A. Jamalipour, M. Katayama, and A. Ogawa. Traffic characteristics of LEOS-based global personal communications networks. *IEEE Communications Magazine*, February 1997.

[9] A. Jamalipour, M. Katayama, T. Yamazato, and A. Derroni. A performance analysis on the effects of traffic non-uniformity in low earth-orbit satellite communication systems. In *SITA*, 1993.

[10] Y. S. Kim, Y. H. Bae, Y. Kim, and J. P. Boutes. Traffic load balancing in low earth orbit satellite networks. In *Computer Communications and Networks*, 191-195 1998.

[11] R. Mauger and C. Rosenberg. QoS guarantees for multimedia services on a TDMA-based satellite network. *IEEE Communications Magazine*, pages 56–65, July 1997.

[12] G. Pennoni and A. Derroni. Mobility management in LEO/ICO satellite systems: Preliminary simulation results. In *PIMRC*, pages 1323–1329, 1994.

[13] H. Perros. *Queueing Networks with Blocking: Exact and Approximate Solutions.* Oxford University Press, 1994.

[14] G. Ruiz, T. L. Doumi, and J. G. Gardiner. Teletraffic analysis and simulation of mobile satellite systems. *IEEE Transactions of Vehicular Technology*, 47(1):311–320, February 1998.

[15] H. Uzunalioglu. Probabilistic routing protocols for low earth orbit satellite networks. In *IEEE ICCC*, 1998.

[16] H. Uzunalioglu and W. Yen. Managing connection handover in satellite networks. In *IEEE Globecom*, 1997.

[17] H. Uzunalioglu, W. Yen, and I. F. Akyildiz. A connection handover protocol for LEO satellite ATM networks. In *ACM/IEEE MobiCom '98*, pages 204–214, 1997.

[18] M. Werner. A dynamic routing concept for ATM-based satellite personal communication networks. *IEEE Journal on Selected Areas in Communications*, 15(8):1636–1648, October 1997.

[19] M. Werner, C. Delucchi, H. J. Vogel, G. Maral, and J. J. DeRidder. ATM-based routing in LEO/MEO satellite networks with intersatellite links. *IEEE Journal on Selected Areas in Communications*, 15(1):69–81, January 1997.